Cardiac Myocytes' Dynamic Contractile Behavior Differs Depending on Heart Segment

Emerson J. De Souza,[1] Wylie Ahmed,[1] Vincent Chan,[2] Rashid Bashir,[2] Taher Saif[1]

[1]Department of Mechanical Science and Engineering, University of Illinois at Urbana Champaign, Illinois, 142 MEB MC: 244, 1206 W. Green Street, Urbana, Illinois 61801; telephone: 217-333-0958; fax: 217-244-9980; e-mail: emerson.jose.desouza@gmail.com

[2]Department of Micro and Nanotechnology, University of Illinois at Urbana Champaign, Illinois, Urbana, Illinois

ABSTRACT: Cardiac myocytes originating from different parts of the heart exhibit varying morphology and ultrastructure. However, the difference in their dynamic behavior is unclear. We examined the contraction of cardiac myocytes originating from the apex, ventricle, and atrium, and found that their dynamic behavior, such as amplitude and frequency of contraction, differs depending on the heart segment of origin. Using video microscopy and high-precision image correlation, we found that: (1) apex myocytes exhibited the highest contraction rate (∼17 beats/min); (2) ventricular myocytes exhibited the highest contraction amplitude (∼5.2 micron); and (3) as myocyte contraction synchronized, their frequency did not change significantly, but the amplitude of contraction increased in apex and ventricular myocytes. In addition, as myocyte cultures mature they formed contractile filaments, further emphasizing the difference in myocyte dynamics is persistent. These results suggest that the dynamic behavior (in addition to static properties) of myocytes is dependent on their segment of origin.

Biotechnol. Bioeng. 2012;xxx: xxx–xxx.

© 2012 Wiley Periodicals, Inc.

KEYWORDS: cardiac tissue engineering; cell transplantation; heart physiology; sarcomere length; myocyte filament

Introduction

The heart consists of many types of cells and their properties vary depending on their spatial location (e.g., pacemaker, conducting tissues, atrial and ventricular walls, etc.) (Barnett, 2005a; Laske and Iaizzo, 2005; Opie, 2004). It is well known that morphology and structure of cells in the heart differ and this has driven studies of heart shape and size for over a century (Burton, 1957; Kyrieleis, 1963; Thomson, 1896).

For instance, the duration of action potentials is different in atrium, ventricle, and Purkinje fibers with values of 150, 250, and 300 ms, respectively (Barnett, 2005b; Laske and Iaizzo, 2005). Right and left apex has been distinguished by increase of its surface area and relative cell alignment during heart looping (Manasek et al., 1972). Electromechanical coupling demonstrated that increased contraction force following an increase in stimulation frequency was significantly higher in atrium than in ventricle (Schwinger, 1993). Pacing at the right ventricular apex adversely affects hemodynamics, while pacing at the left ventricular septum or apex causes best function because pacing from these sites creates a physiological propagation of electrical conduction (Peschar, 2003). Atrial and ventricle myocardium have shown different mechanism of force generation in response to external stretching (Kockskämper et al., 2008).

The examples above display the relationship between regions of the heart and heart function at the full organ level (1936; Barnett, 2005b; Burton, 1957; Kockskämper et al., 2008; Kyrieleis, 1963; Manasek et al., 1972; Peschar, 2003; Schwinger, 1993; Thomson, 1896), while studies in the 1950s and 1960s revealed the importance of understanding the individual myocyte behavior for the full organ function (Burton, 1957; Kyrieleis, 1963). The relationship between individual myocytes and the full organ became the motivation to continue investigating different segments of heart tissues (Kockskämper et al., 2008; Legato, 1970; Schwinger, 1993; Sommer and Johnson, 1968), to distinguish individual myocytes (Manasek et al., 1972; Silver et al., 1983), and to measure the force at the cellular level (Jacot et al., 2010; Linder et al., 2010). In the context of individual myocytes in vitro, the contraction rate and amplitude of myocardial cells became fundamental observables, because they allow the extraction of mechanical and biochemical information between myocytes and their microenvironment. Engler et al. (2008) has shown, for example, that

myocardial cells beat with higher frequency on soft substrates than on hard substrates. They interpreted that hardening of the heart during myocardial infarction can lead to a cascade of effects causing healthy cells not to beat. More recently the effect of matrix and substrate stiffness on single myocytes has been investigated to study cellular behavior in injured myocardium (Bhana et al., 2010; Engler et al., 2008; Shapira-Schweitzer and Seliktar, 2007).

In summary, earlier studies at the full organ level demonstrated how spatial organization and varying morphology collectively result in the dynamical behavior of the heart and ultimately affects its function. Likewise, previous investigations have shown that the morphology and ultrastructure of atrial and ventricular myocytes are different, but the difference of the dynamical behavior of individual myocytes in vitro has not been studied yet. In the last decade, there has been significant interest in myoblast and myocyte transplantation (Taylor et al., 1998; Zimmermann, 2006), scaffold injection (Leor, 2000; Ott et al., 2008), and bioengineered myocardium tissue (Carrier et al., 1999; Dengler et al., 2011; Zimmermann and Eschenhagen, 2003; Zimmermann et al., 2000), as potential candidates for repairing heart failure. As research in these fields progress, it is important to understand that myocytes from different regions of the heart behave dynamically different.

Often, studies that use neonatal rat ventricular myocytes remove the atria prior to isolation as they are very easy to distinguish and remove in the neonatal rat heart. In this paper, the tissue of each heart segment is millimetrically isolated exactly following earlier procedures (Laks et al., 1967). Myocytes were extracted from the atrium, ventricle, and apex, to investigate if their behavior was dependent on their segment of origin. Cells were observed using video microscopy and image correlation was used to evaluate contraction rate and amplitude as the cultures evolved in time. As an analogy to the electrocardiogram, which displays electrical activity at the full organ level, we present a displacement myocytogram (DMG), which displays the dynamic behavior of myocytes in vitro.

Materials and Methods

Cell Extraction and Culture

Cardiomyocytes were obtained from 5-day-old Sprague-Dawley rats (Harlan Laboratories Inc., Indianapolis, IN) (IACUC; Protocol No. 08190). The hearts of only female rats were used in this study to exclude variation due to gender (Buñag and Davidow, 1996). The heart was excised from the rat (Maass and Buvoli, 2007) and immediately placed in ice-cold Hanks' Balanced Salt Solution (HBSS) (1X), (Invitrogen Corp., Grand Island, NY, Cat. No. 14175-095) buffer (Fig. 1a). The heart was then cut along the inter-ventricular septum (Fig. 1b) and the left and right walls were separated. The left tissue was then further cut into five segments for the cell extraction as described below (Fig. 1d).

Three tissue segments 1, 3, and 5 (Fig. 1d) from apex, ventricle, and atrium, respectively, were individually digested in 0.05% (w/v) purified trypsin (Worthington Biochemicals Corp., Lakewood, NJ, Catalogue No. LS003734), while rotating gently at 4°C overnight. After 16 h, warm growth medium was added for 5 min at 37°C to inhibit trypsin digestion. After washing and discarding the supernatant, 0.1% (w/v) purified type II collagenase (Worthington Biochemicals Corp., Catalogue No. LS004176) was added for 45 min while rotating at 37°C. The tissue was gently triturated to mechanically loosen the cells, and the suspension was filtered through a 40-μm cell strainer. The suspension was removed after centrifugation at 150g for 6 min. The remaining cell pellet of each segment of the heart was re-suspended in warm growth medium and pre-plated for 1 h to enrich for cardiomyocytes. The suspension was collected, and cardiomyocytes of different segments from the left side of the heart were seeded on polystyrene dishes. The growth medium consisted of high glucose DMEM (Invitrogen Corp., Grand Island, NY, Catalogue No. 31053028) with 10% fetal bovine serum. The cells were cultured in an incubator with 5% CO_2 at 37°C.
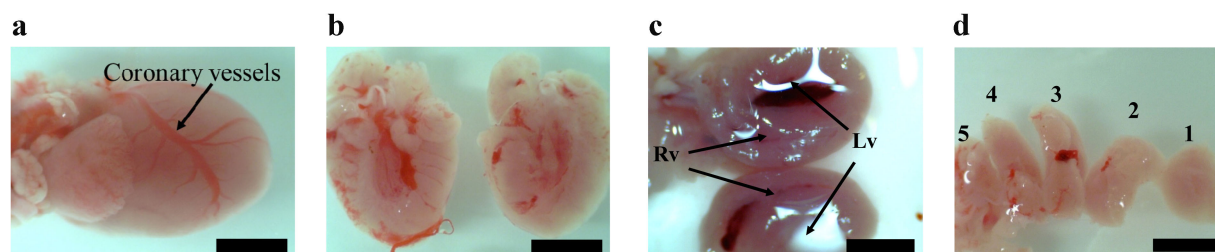

Figure 1. **a**: Image of the entire heart immersed in HBSS at 4°C (20 min after dissection). In this anterior view of the heart, the coronary vessels are visible as indicated by arrows. The left anterior descending is used as a guide to precisely cut the heart either along or across the inter-ventricular septum. **b**: A cut along the inter-ventricular septum exposes the left (Lv) and right (Rv) ventricles, respectively. **c**: A cut across the inter-ventricular septum shows a cross-section of the Lv and Rv in both halves. **d**: The Lv is separated into multiple segments for cell extraction. From left to right: (5) atrium, (3) ventricle, (1) apex are used for cell extraction and the extra tissues (4 and 2) are not used to provide isolation between the segments (scale bar = 3 mm).

Isolating Different Segments of the Heart

The two heart chambers were separated immediately after the animal was euthanized. This method was preferred since cutting along the inter-ventricular septum (Fig. 1b) was easier while the heart was still beating, connected to the lungs and the dark color of the right ventricle was visible. Figure 1c shows the cross-section of both ventricular cavities when the heart is cut across the septum. Following the previous literature (Opie, 2004), the left side of the heart exerts most of the work to pump the oxygen-rich blood into the body. Therefore, we assumed that the tissue from the left side is a convenient choice to display the differences between the myoyctes and the cells were extracted from the left atrium, left ventricle, and left apex.

The length of the entire heart varies between 4 and 7 mm (see Fig. 1a–d) and the heart tissue behaves like a soft gelatin covered with a strong skin. Therefore, cutting the heart with millimetrical precision is an approach that requires good visualization. To allow precise imaging while dissecting the segments of the heart, a micro digital camera (Dnt-Mikroskopkamera-Digimicro-2.0, Drahtlose Nachrichtentechnik Entwicklungs- und Vertriebs GmbH, Dietzenbach, Germany) was used in the sterilized culture hood. The working distance was sufficiently large to easily manipulate the dissection scissors and the magnification of $10\times$ enabled viewing of the entire heart on a computer monitor outside the hood. The high accuracy of the segment cuts yields high consistency in segment weights, which results in well-controlled concentration of myocytes from different segments. The left side of the heart was separated into five pieces (Fig. 1d) and segments 1, 3, and 5 were used for cell extraction. The exclusion of segments 2 and 4 was necessary to avoid using cells from neighboring segments and ensure isolation of cells from distinctly different segments of the heart.

Microscopy and Image Processing

All images were collected using phase contrast optics on an Olympus IX-81 microscope (Olympus America Inc., Melville, NY) using a $20\times$ objective and videos were recorded at 72 frames/s. Image processing was done via MATLAB (The MathWorks, Natick, MA) (Bister, 2007; Zuria et al., 1998) and statistical analysis was computed in Origin (OriginLab Corporation, Northhampton, MA). To track the myocyte contraction, we introduce the DMG. The DMG is a graphical representation of myocyte contraction as a function of time. To create the DMG, cellular contraction was quantified by applying an image correlation toolbox from Matlab that enables displacement tracking of each pixel in x and y directions and thus yields two-dimensional displacement of all pixels generated by contractile myocytes between frames of the video. We use the displacement of each pixel in the image sequence to obtain the contraction rate (reported as beats per min [bpm]) and the contraction amplitude (μm). Figure 2a shows one frame extracted from a video (see video of an apexial myocyte contraction in supplemental material) and Figure 2b shows a representative scalar field of contraction amplitudes. To show the direction of contraction, a vector field is reconstructed and shown in Figure 2c. The pixel displacements in the x and y directions were then used to calculate the total displacement via $(x^2 + y^2)^{1/2}$. The total displacement of single myocytes as a function of time is represented in the DMG's below (Fig. 3). When multiple myocytes beat simultaneously, they are labeled as synchronous (Gaudesius et al., 2003; Glass et al., 1983). The synchronization is defined as the simultaneous contraction and relaxation of multiple myocytes as a function of time independent on the value of their amplitudes.

Results

Myocyte Concentration and Evolution of Cell Culture

All cardiac tissues have been weighted prior to the digestion in trypsin and their weights approached (20.05 ± 2.42 mg) for each segment ($n = 24 = 3$ segments $\times$ 8 hearts). Before the cells were plated; they were counted for accurate control of cell concentration. The typical myocyte concentration for the suspension of any segment was fixed to 42 ± 8 myocyte/mm^2. This low concentration was necessary to precisely distinguish and follow the dynamics of individual myocytes during contraction in vitro.

Spontaneous contraction for a small number of myocytes was observed 24 h after cell plating in cultures from all heart segments (rate < 6 bpm). Due to the difficulty of finding dynamically active myocytes at this age of culture no video was recorded. This strategy was used to avoid the unnecessary exposure of the cultures outside the incubator. At this early culture stage, cells debris and tissue fragments strongly adhered to the substrate and made the counting of myocytes per area inaccurate. By the second day of culture, myocytes contracted independently from each other and fibroblasts showed significant spreading. Contracting myocytes were not as rare as they were found for the first day. The beating rate was still very low and irregular making extraction of meaningful parameters from the recorded videos difficult. The typical density of *contractile myocytes* was 25 ± 5 cells/mm^2 for any segment, which equals 60% of 42 ± 8 cells/mm^2 prior to plating the cells. This means that about 40% of the counted items from the suspension were not contractile myocytes. This concentration was estimated by recording five different images and each image contained between 4 and 6 myocytes. Since the amount of cells for each segment was controlled prior to plating, the density did not depend on the origin from the heart. The typical cell–cell separation for this concentration was about 110 ± 25 μm. This cell density and separation was observed in all videos recorded for the experiments below. By Day 4 of culture, the average rate increased to 10 bpm and became segment dependent. The myocytes still contracted independently from neighboring cells and five videos were recorded in positions 3 mm apart from each other. Five videos of each
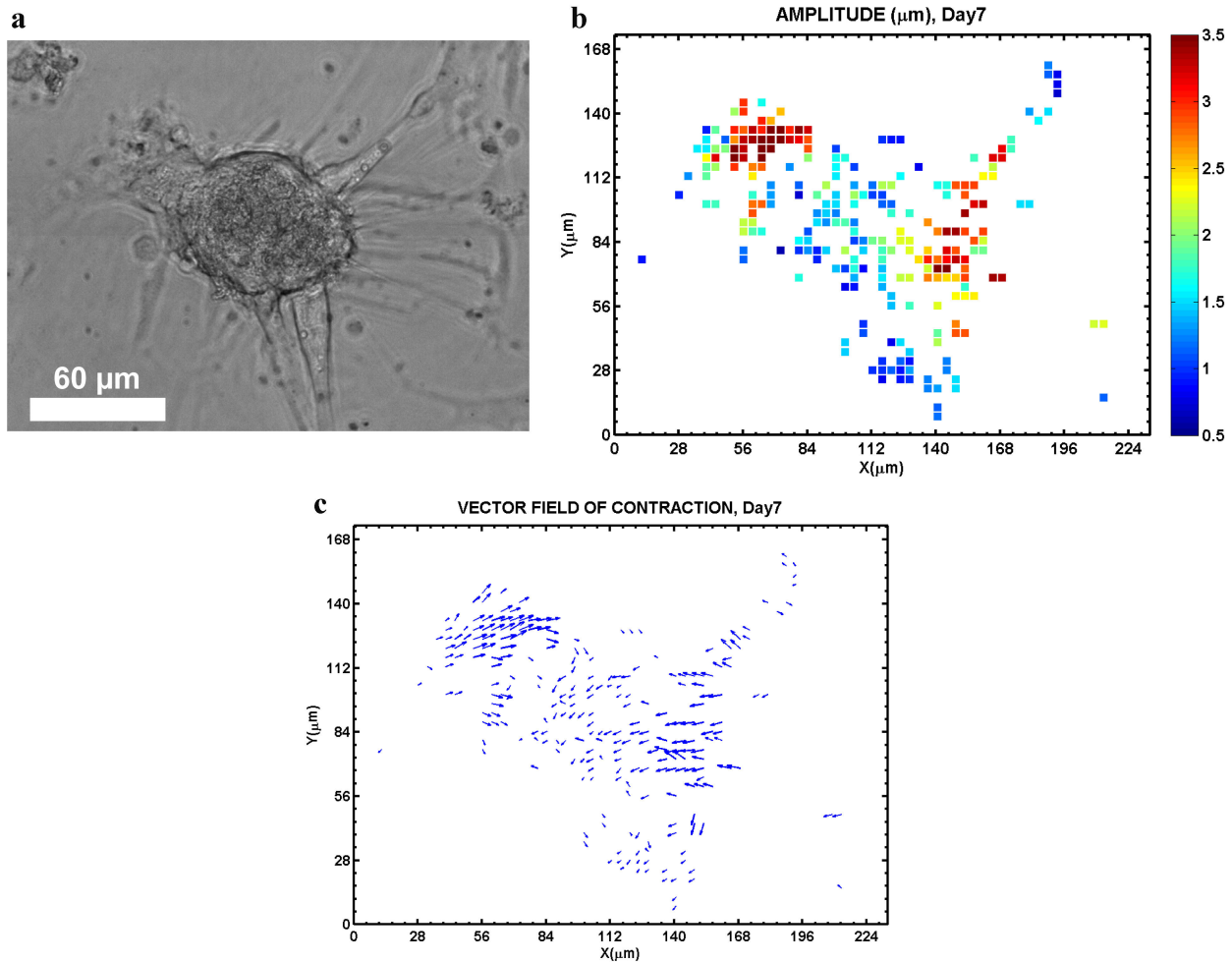
Figure 2. **a**: One frame is extracted from the video-microscopy (see video of myocyte contraction in supplemental material) to illustrate the morphology of an isolated apexial myocyte. The dimensions of the frame are 232 × 174 μm. **b**: The total amplitude of myocyte contraction is obtained from x_and y_displacements via $(x^2 + y^2)^{1/2}$ and are displayed as scalar field. **c**: The vector field of myocyte contraction displays the direction of motion of the myocytes within the entire frame. The displacements are not obtained from edge detection methods but from tracking the displacements in x and y directions of every pixel.

heart segment were collected. Simultaneous contractions of individual myocytes were visible at the fifth day if the cell density was larger than seven myocytes per $400 \, \mu m^2$. This had happened occasionally but most of the contraction and relaxation still occurred independently. At the sixth day of cell culture, the beat of one myocyte occurred simultaneous to the contraction of another myocyte and all cells contracted and relaxed at the same time.

Myocyte Dynamics Differ Depending on Heart Segment

By Day 4 of culture, myocytes exhibited different contraction behavior depending on the originating segment of the heart as shown by the representative DMGs in Figure 3 and the statistics in Figure 4. Myocytes from the apex exhibited the highest contraction rate (∼17 bpm) while myocytes of the ventricle (∼11 bpm) and atrium (∼12 bpm) contract

with two-third the rate of the apex ($P < 0.05$). Conversely, myocytes from the apex exhibited the lowest contraction amplitude (∼1.6 micron) while myocytes of the ventricle (∼2.8 micron) and atrium (∼2.7 micron) contracted significantly more ($P < 0.05$). These results show that myocytes from different segments of the heart exhibit significantly different dynamic behavior.

Synchronized Cells Exhibit Larger Contraction

By Day 6 of culture, myocytes began to show synchronized contractile behavior. Interestingly, synchronized cells of the ventricle and apex show contraction amplitudes significantly larger in comparison to their independent beating on Day 4 (Fig. 4). Myocytes from the apex exhibited an increase in contraction amplitude from 1.6 to 3.8 micron while maintaining the same contraction rate (∼17 bpm).
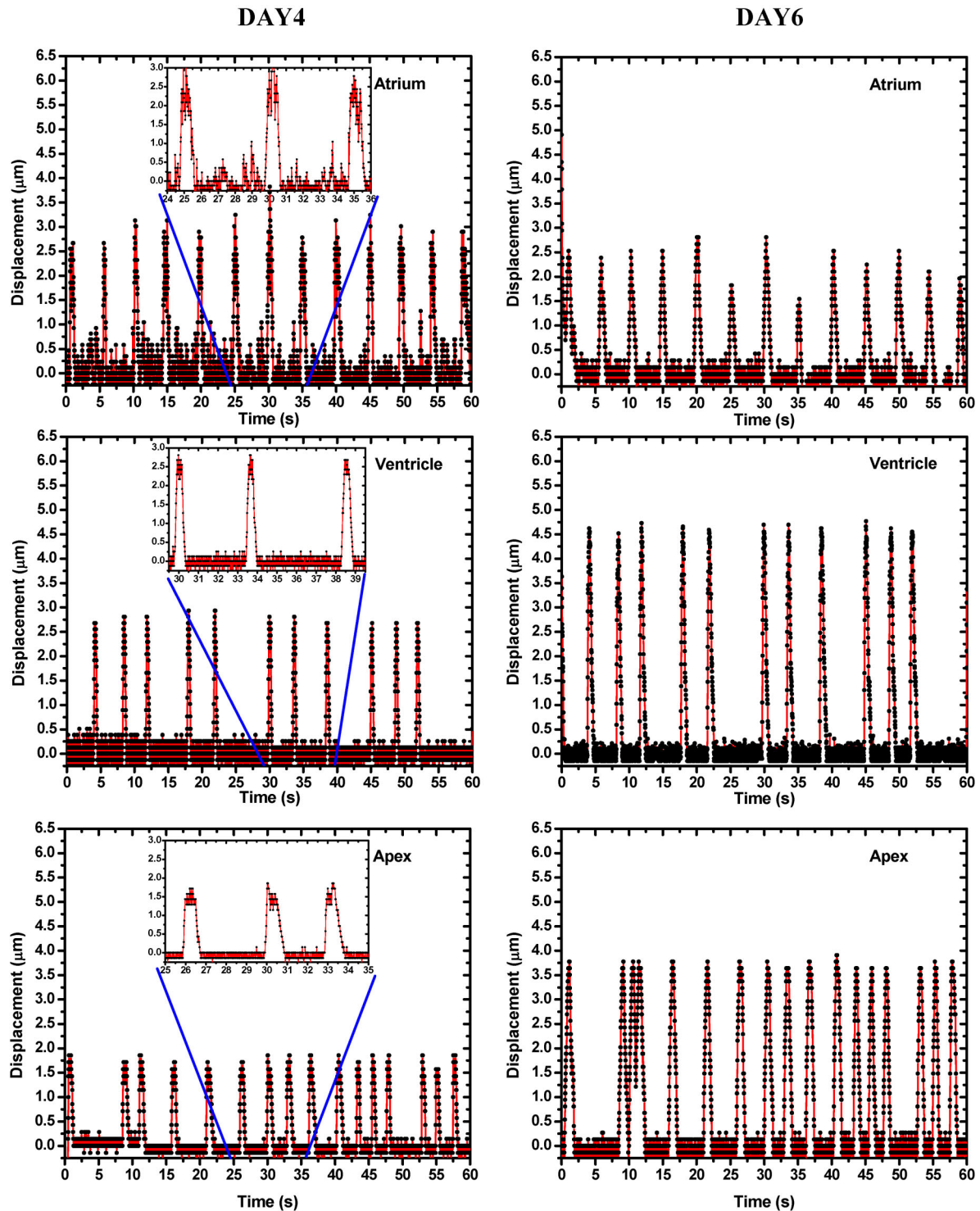
Figure 3. Representative DMGs of atrial, ventricular, and apexial myocytes for cell cultures on Day 4 (left) and Day 6 (right) of culture. Notice the large change in contraction amplitude for myocytes of the apex and ventricle by Day 6 when cells beat synchronously.

Ventricular myocytes showed an increase in contraction amplitude from 2.8 to 5.2 micron and also showed a slight increase in beating rate from 11 to 12 bpm ($P < 0.05$). Atrial myocytes exhibited no significant change in their

contraction amplitude or rate after synchronization. Representative DMGs are shown in Figure 3 and statistical results are summarized in Figure 4. These results show that the time evolution of myocyte contractile behavior is
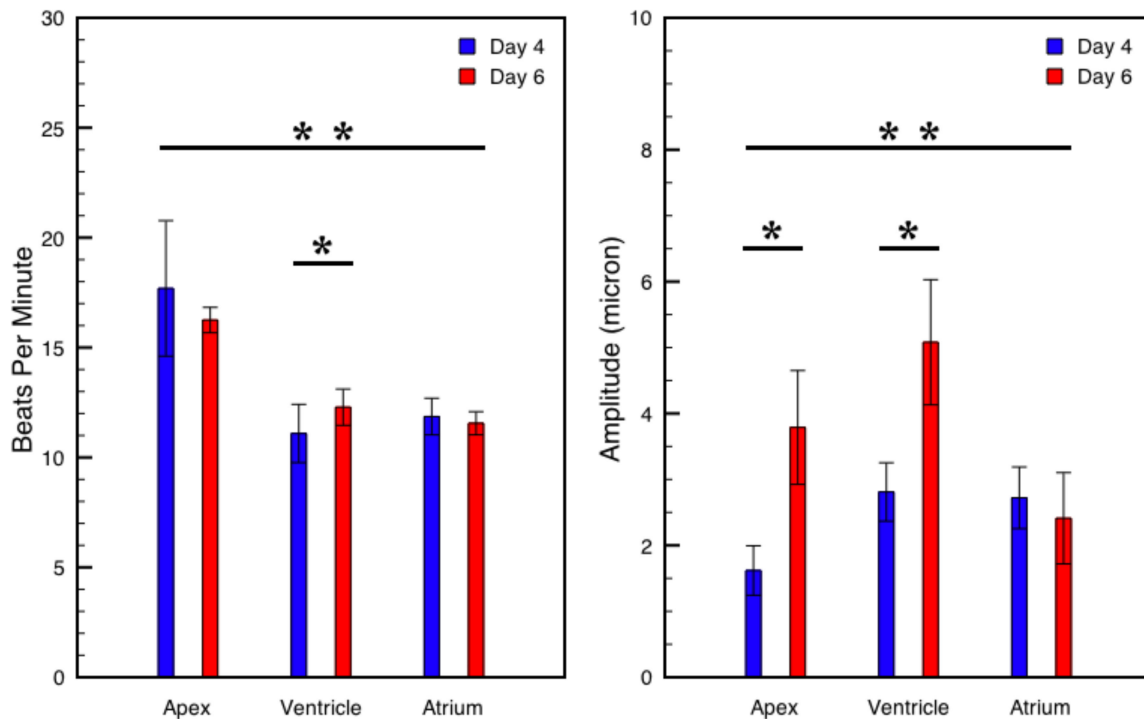
Figure 4. Charts summarizing the dynamic behavior of myocytes from different segments of the heart. **a**: The average bpm of cells from different segments were significantly different ($P < 0.05$). Myocytes of the ventricle ($n = 21$) showed a significant increase in BPM from Day 4 to 6 ($P < 0.05$), which was not observed in cells of the apex ($n = 15$) and atrium ($n = 14$). **b**: The average contraction amplitude significantly differed between cells from all segments ($P < 0.05$). Myocytes of the apex ($n = 15$) and ventricle ($n = 21$) showed a significant increase in contraction amplitude ($P < 0.05$) after the onset of synchronized beating (Day 6) (error bars = SD).

dependent on the segment of origin. The cell density or confluency changes the rate and the amplitude of contraction of any type of myocyte (Orita, 1993). The dependence of rate on myocyte density and confluency (or age of culture) is discussed below. However, the rigorous control of cell density described in the methods and the simultaneous observation of the events allow us to exclude these parameters in our comparison. The myocyte density of all segments is identical and the confluency of cell at any age of culture did not display observable differences.

Discussion

The morphology and ultrastructure of myocytes is segment dependent (Laks et al., 1967; Legato, 1973; McNutt and Fawcett, 1969; Moses and Claycomb, 1984; Urthaler et al., 1978). Using DMGs, our results show that the dynamics of in vitro myocyte contraction are also segment dependent.

Dynamics of Cardiac Myocytes

The dynamics of general myocyte contraction have been investigated previously (Kamgoué et al., 2009; Linder et al.,

2010; Pustoc'h et al., 2005), but direct comparisons with the present study is difficult due to differences in the cellular micro-environment and analysis techniques. Trzewik et al. (Linder et al., 2010), cultured myocyte monolayers on flexible membranes and measured their contraction rate and the stress/strain in the membrane. The observed beating rate of over 200 bpm was significantly higher than the beating rate of 10–18 bpm observed in the present study. This is not surprising since in the previous experiments myocyte density and culture age were much higher, and both factors are known to contribute to increased beating rate (Orita, 1993). Videos of metronome oscillations were recorded to validate our method. In this experiment, the frequency and the amplitude of the metronome were varied. Then, the digital image correlation method, used to track the contraction of myocytes, was applied to track the oscillation of metronomes. It was verified that the frequency and amplitude of input were identical to the frequency and amplitude of output obtained from the DMG-technique. This validation of the method is not included because the focus of this study is on the differences between the myocytes rather than characterization of the technique. Furthermore, contraction rates of approximately 300 bpm have been observed using the same tracking method but for myocyte culture with higher cell concentration. Therefore,

the large difference in rate observed in previous studies (Linder et al., 2010) may be attributed to the concentration and age of culture and is unlikely an artifact due to the method used. The system developed by Trzewik et al. (Linder et al., 2010) was intended to study myocyte monolayers under biaxial loading. The CellDrum technology offers many possibilities for in vitro investigations on cardiac function, but does not allow investigations of the dynamics of individual myocytes. Thus changes in contraction rate and amplitude of individual cells during synchronization cannot be studied by the method from Trzewik et al.

Pustoc'h et al. (2005) obtained a contraction rate of 3–4 bpm with an amplitude of 8 μm for individual myocytes. Their values were determined from snapshots of time-lapse video-microscopy recorded at 9 frames/s (fps). The difference between their values with our results could be due to the lower recording rate of 9 fps compared with 72 fps in this study. Information of cell density and culture age was not given. The frame rate at which videos are recorded dramatically impacts the observation of the actual event. For the particular case of myocyte contraction, if the pulse length of contraction and relaxation (not the bpm) is fast compared with the recording rate, the video camera does not record the complete event and fewer contractions per minute can be observed during the video. For example, if the pulse length is half second, the recording rate of 9 fps will record only four images and will eventually not be enough to display the entire movement. The peak may be lost and only a small vibration displaying the start and the end of contraction may be observed. We did experiments with different sampling rates prior to the videos recorded for this paper and confirmed the statements above. Further, environmental effects such as temperature, CO_2 level, cell media, etc, are also known to affect the contraction rate of myocytes (Langer et al., 1999).

Later, Kamgoué et al. (2009) developed a technique to study the contraction rate and amplitude of individual myocytes based on digital image correlation. Their method enabled a quantitative analysis of cardiac myocyte contraction without requiring specific markers, such as micro-beads or the use of fluorescent calcium probes (Balaban et al., 2001; Dembo and Wang, 1999). However, their algorithm did not allow sub-pixel tracking accuracy and their temporal resolution were limited to their sampling rate of image acquisition.

Segment Dependence of Cardiac Myocyte Dynamics

Previous studies of myocyte dynamic behavior have not focused on segment dependence. It is therefore unclear if the previously observed high contraction rate (Linder et al., 2010; Orita, 1993) would also occur in separate cultures of myocytes from different segments of the heart. It is expected that the rate of any type of myocyte will converge to rates of 300 bpm if the concentration of myocytes is sufficiently high and the culture is sufficiently adult because the entire neonatal heart pumps synchronized at roughly 300 bpm before the dissection (Buñag and Davidow, 1996). However, it is unclear how myocytes from apex, ventricle, and atrium will evolve to convergence under low concentration and how the differences between them will depend as a function of culture age. Future studies should investigate if behavior that is characteristic of general myocyte cultures will still occur in myocytes isolated from different segments. For instance, change of beating rate and acceleration of hypertrophy are characteristics of differentiation and growth of myocytes during the neonatal period (Orita, 1993), but it is unclear if this behavior persists in isolated segments of the heart. Such studies may allow a deeper understanding of cellular organization and provide a basis for engineering cells and tissues for cardiac repair.

In this study, we have presented the use of DMGs to quantify the dynamic behavior of myocytes from different segments of the heart. The DMGs provide information regarding beating rate, amplitude, and synchronization. The sub-pixel accuracy of the tracking method combined with higher temporal resolution by utilizing a higher frame rate for image acquisition extends the tracking procedure proposed by Kamgoué et al. (2009). The present technique is particularly useful since it can be applied to analyze any sequence of images and is independent of the specific experimental setup. By utilizing DMGs, future studies allow investigating the segment dependence of beating rate acceleration (Orita, 1993) and contractile synchronization with time (Gaudesius et al., 2003; Glass et al., 1983). Investigations of these parameters will help to understand how cells from different segments of the heart differ dynamically, which is crucial to studies of cardiac regeneration therapy.

Filament Formation

To illustrate the importance of segment dependent behavior, here we discuss an example of persistent differences in myocyte dynamics as cultures mature with time. Atrial and ventricular myocytes were monitored over a period of 2 months. Interestingly, ventricular myocytes detached from the underlying substrate and formed contractile filaments by Day 21, while atrial myocytes remained well adhered to the substrate as shown in Figure 5a and b (see also the videos: 2_ventricular_filament and 3_sticky_atrial in supplemental material). The contraction rate of 125 bpm for ventricular filaments was significantly increased compared with the rate of 12 bpm at Day 6. Similarly, the amplitude of contraction increased up to displacements of 60 μm or a factor of 12 times larger than the amplitudes prior to the formation of filament structure. The contraction rate and amplitude of atrial myocytes at the Day 21 did not change at all relative to the Day 6. With progressing evolution of both cultures, the ventricular filaments ruptured and stopped contraction (1 month of culture age) while atrial myocytes evolved slowly
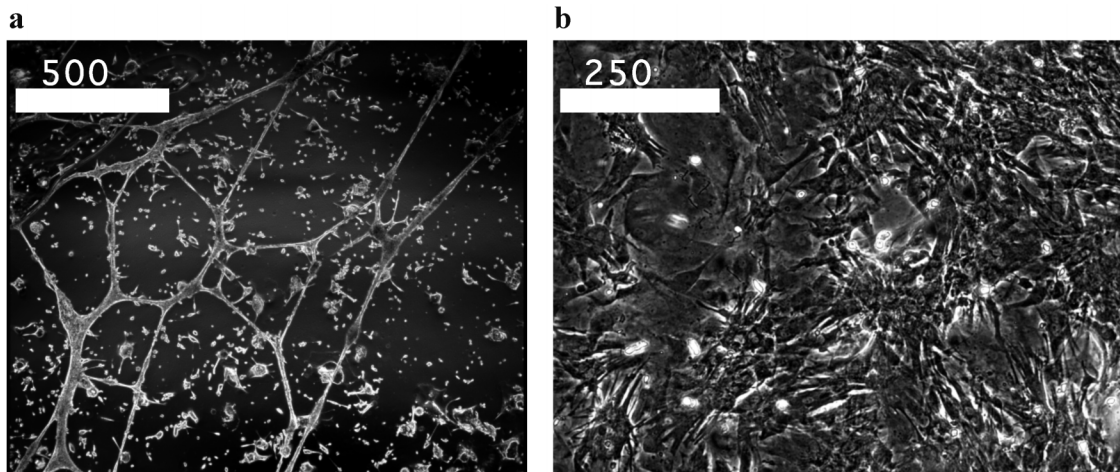
Figure 5. **a**: Displays the formation of ventricular filaments and **b**: Displays an atrial myocyte culture still adhered to the substrate. The frames were extracted from the video-microscopy (see videos: 2_ventricular_filament and 3_sticky_atrial in supplemental material). Both videos were recorded on Day 21 of culture.

and eventually formed contractile filaments 1 month later than the ventricular ones. This observation was obtained from multiple parallel cultures (n = 7) of ventricular and atrial myocytes. The formation and time evolution of the contractile filaments is currently under investigation and will be explored in depth for a future publication. This example of differing dynamics in aging cultures suggests that myocytes from different segments are intrinsically different and these differences persist as cultures mature.

Contraction Amplitude and Sarcomere Length

Sarcomere length is segment dependent (Laks et al., 1967) and could give rise to segment dependent intracellular stress (Weiwad et al., 2000). This force dependence on sarcomere length is a possible mechanism to explain the change in contractile properties with heart segment as well as culture age. For instance, one model (Tracqui et al., 2008) suggests that myocytes with a larger initial sarcomere length have an increased regime of stretching in which they are able to generate large forces resulting in large contraction amplitudes. Ventricular myocytes have a larger sarcomere length than myocytes from other segments (Laks et al., 1967), which is consistent with their larger contraction amplitude. In addition, external tension in the culture increases with culture age (Trzewik et al., 2004), which may affect the sarcomere length and subsequently change contraction amplitude with time. For in-depth studies of the sarcomere–tension relationship, experimental measurements of sarcomere length and external tension of myocytes in vitro are necessary. However, based on previous measurements of myocyte ultrastructure (Laks et al., 1967), the sarcomere–tension relationship suggests a possible mechanism for the

segment dependence of dynamic behavior in cardiac myocytes.

Clinical Relevance and Conclusion

Our study shows, for the first time, that myocytes from different segments of the heart are dynamically different in their contraction frequency and amplitude. Cell-based regenerative therapy and engineered myocardiac tissue should consider the source of myocyte origin from within the heart. Recent advances in cardiac therapy and engineering have shown great promise (Murry, 2005; Ott et al., 2008), however, significant progress must be made to be clinically viable. Understanding the dynamic behavior of different cell types for regenerative therapy might be crucial for their functional integration with native tissues.

References

Balaban NQ, Schwarz US, Riveline D, Goichberg P, Tzur G, Sabanay I, Mahalu D, Safran S, Bershadsky A, Addadi L, Geiger B. 2001. Force and focal adhesion assembly: A close relationship studied using elastic micropatterned substrates. Nat Cell Biol 3(5):466–472.

Barnett VA. 2005a. Cardiac myocytes. In: Iaizzo PA, editor. Handbook of cardiac anatomy, physiology, and devices. Totowa, NJ: Humana Press. p 73–76.

Barnett VA. 2005b. Cardiac myocytes. In: Iaizzo PA, editor. Handbook of cardiac anatomy, physiology, and devices. Totowa, NJ: Humana Press. p 113–121.

Bhana B, Iyer RK, Chen WLK, Zhao R, Sider KL, Likhitpanichkul M, Simmons CA, Radisic M. 2010. Influence of substrate stiffness on the phenotype of heart cells. Biotechnol Bioeng 105(6):1148–1160.

Bister M. 2007. Increasing the speed of medical image processing in MatLab®. Biomed Imaging Intervent J 3(1):1–12.

Buñag RD, Davidow LW. 1996. Aging impairs heart rate reflexes earlier in female than in male Sprague-Dawley rats. Neurobiol Aging 17(1):87–93.

Burton AC. 1957. The importance of the shape and size of the heart. Am Heart J 54(6):801–810.

Carrier RL, Papadaki M, Rupnick M, Schoen FJ, Bursac N, Langer R, Freed LE, Vunjak-Novakovic G. 1999. Cardiac tissue engineering: Cell seeding, cultivation parameters, and tissue construct characterization. Biotechnol Bioeng 64(5):580–589.

Dembo M, Wang YL. 1999. Stresses at the cell-to-substrate interface during locomotion of fibroblasts. Biophys J 76(4):2307–2316.

Dengler J, Song H, Thavandiran N, Massé S, Wood GA, Nanthakumar K, Zandstra PW, Radisic M. 2011. Engineered heart tissue enables study of residual undifferentiated embryonic stem cell activity in a cardiac environment. Biotechnol Bioeng 108(3):704–719.

Engler AJ, Carag-Krieger C, Johnson CP, Raab M, Tang HY, Speicher DW, Sanger JW, Sanger JM, Discher DE. 2008. Embryonic cardiomyocytes beat best on a matrix with heart-like elasticity: Scar-like rigidity inhibits beating. J Cell Sci 121(22):3794–3802.

Gaudesius G, Miragoli M, Thomas SP, Rohr S. 2003. Coupling of cardiac electrical activity over extended distances by fibroblasts of cardiac origin. Circ Res 93(5):421–428.

Glass L, Guevara MR, Shrier A, Perez R. 1983. Bifurcation and chaos in a periodically stimulated cardiac oscillator. Phys D Nonlin Phenomena 7(1–3):89–101.

Jacot JG, Kita-Matsuo H, Wei KA, Vincent Chen H, Omens JH, Mercola M, McCulloch AD. 2010. Cardiac myocyte force development during differentiation and maturation. In: Braaten D, editor. Annals of the New York Academy of Sciences: Analysis of cardiac development: from embryo to old age. New York: Blackwell Publishing Inc. p 121–127.

Kamgoué A, Ohayon J, Usson Y, Riou L, Tracqui P. 2009. Quantification of cardiomyocyte contraction based on image correlation analysis. Cytometry Part A 75A(4):298–308.

Kockskämper J, von Lewinski D, Khafaga M, Elgner A, Grimm M, Eschenhagen T, Gottlieb PA, Sachs F, Pieske B. 2008. The slow force response to stretch in atrial and ventricular myocardium from human heart: Functional relevance and subcellular mechanisms. Prog Biophys Mol Biol 97(2–3):250–267.

Kyrieleis C. 1963. The changes in the shape of the human heart after birth. Die Formveränderungen des menschlichen Herzens nach der Geburt 337(2):142–163.

Laks MM, Nisenson MJ, Swan HJ. 1967. Myocardial cell and sarcomere lengths in the normal dog heart. Circ Res 21(5):671–678.

Langer SFJ, Lambertz M, Langhorst P, Schmidt HD. 1999. Interbeat interval variability in isolated working rat hearts at various dynamic conditions and temperatures. Res Exp Med 199(1):1–19.

Laske TG, Iaizzo PA. 2005. The cardiac conduction system. In: Iaizzo PA, editor. Handbook of cardiac anatomy, physiology, and devices. Totowa, NJ: Humana Press. p 123–136.

Legato MJ. 1970. Sarcomerogenesis in human myocardium. J Mol Cell Cardiol 1(4):425–432. IN13–IN41, 433–437.

Legato MJ. 1973. Ultrastructure of the atrial, ventricular, and Purkinje cell, with special reference to the genesis of arrhythmias. Circulation 47(1):178–189.

Leor J. 2000. Bioengineered cardiac grafts: A new approach to repair the infarcted myocardium? Circulation 102(19):III56–III61.

Linder P, Trzewik J, Rüffer M, Artmann G, Digel I, Kurz R, Rothermel A, Robitzki A, Temiz Artmann A. 2010. Contractile tension and beating rates of self-exciting monolayers and 3D-tissue constructs of neonatal rat cardiomyocytes. Med Biol Eng Comput 48(1):59–65.

Maass AH, Buvoli M. 2007. Cardiomyocyte preparation, culture, and gene transfer. In: Zhang J, Rokosh G, editors. Methods in molecular biology, cardiac gene expression: Methods and protocols. Totowa, NJ: Humana Press Inc. p 321–330.

Manasek FJ, Burnside MB, Waterman RE. 1972. Myocardial cell shape change as a mechanism of embryonic heart looping. Dev Biol 29(4):349–371.

McNutt NS, Fawcett DW. 1969. The ultrastructure of the cat myocardium. II. Atrial muscle J Cell Biol 42(1):46–67.

Moses RL, Claycomb WC. 1984. Ultrastructure of cultured atrial cardiac muscle cells from adult rats. Am J Anat 171(2):191–206.

Murry CE. 2005. Cell-based cardiac repair reflections at the 10-year point. Circulation 112(20):3174–3183.

Opie LH. 2004. Heart cells and organelles. In: Opie LH, editor. Heart physiology: From cell to circulation. 4, Illustrated ed. Philadelphia, PA: Lippincott Williams & Wilkins. p 42–69.

Orita H. 1993. Modulation of cardiac myocyte beating rate and hypertrophy by cardiac fibroblasts isolated from neonatal rat ventricle. Jpn Circ J 57(9):912–920.

Ott HC, Matthiesen TS, Goh SK, Black LD, Kren SM, Netoff TI, Taylor DA. 2008. Perfusion-decellularized matrix: Using nature's platform to engineer a bioartificial heart. Nat Med 14(2):213–221.

Peschar M. 2003. Left ventricular septal and apex pacing for optimal pump function in canine hearts. J Am Coll Cardiol 41(7):1218–1226.

Pustoc'h A, Ohayon J, Usson Y, Kamgoue A, Tracqui P. 2005. An integrative model of the self-sustained oscillating contractions of cardiac myocytes. Acta Biotheor 53(4):277–293.

Schwinger RHG. 1993. Force-frequency-relation in human atrial and ventricular myocardium. Mol Cell Biochem 119(1–2):73–78.

Shapira-Schweitzer K, Seliktar D. 2007. Matrix stiffness affects spontaneous contraction of cardiomyocytes cultured within a PEGylated fibrinogen biomaterial. Acta Biomaterialia 3(1):33–41.

Silver LH, Hemwall EL, Marino TA, Houser SR. 1983. Isolation and morphology of calcium-tolerant feline ventricular myocytes. Am J Phys 245(5 Pt 1):H891–H896.

Sommer JR, Johnson EA. 1968. Cardiac muscle. A comparative study of Purkinje fibers and ventricular fibers. J Cell Biol 36(3):497–526.

Taylor DA, Atkins BZ, Hungspreugs P, Jones TR, Reedy MC, Hutcheson KA, Glower DD, Kraus WE. 1998. Regenerating functional myocardium: Improved performance after skeletal myoblast transplantation. Nat Med 4(8):929–933.

Thomson HC. 1896. The estimation of the size and shape of the heart by the roentgen rays. Lancet 148(3815):1011–1012.

Tracqui P, Ohayon J, Boudou T. 2008. Theoretical analysis of the adaptive contractile behaviour of a single cardiomyocyte cultured on elastic substrates with varying stiffness. J Theor Biol 255(1):92–105.

Trzewik J, Artmann-Temiz A, Linder PT, Demirci T, Digel I, Artmann GM. 2004. Evaluation of lateral mechanical tension in thin-film tissue constructs. Ann Biomed Eng 32(9):1243–1251.

Urthaler F, Walker AA, Kawamura K. 1978. Canine atrial and ventricular muscle mechanics studies as a function of age. Circ Res 42(5):703–713.

Weiwad WKK, Linke WA, Wussling MHP. 2000. Sarcomere length-tension relationship of rat cardiac myocytes at lengths greater than optimum. J Mol Cell Cardiol 32(2):247–259.

Zimmermann WH. 2006. Heart muscle engineering: An update on cardiac muscle replacement therapy. Cardiovasc Res 71(3):419–429.

Zimmermann WH, Eschenhagen T. 2003. Cardiac tissue engineering for replacement therapy. Heart Fail Rev 8(3):259–269.

Zimmermann WH, Fink C, Kralisch D, Remmers U, Weil J, Eschenhagen T. 2000. Three-dimensional engineered heart tissue from neonatal rat cardiac myocytes. Biotechnol Bioeng 68(1):106–114.

Zuria CS, Ramirez JM, Baez-Lopez D, Flores-Verdad GE. 1998. MATLAB based image processing lab experiments. Session S3F, 1998 FIE Conference, p 1255–1258.